A Project Report on

Speckle Reduction and Segmentation in medical Images

Submitted by:

Abhinav Kumar Kushwaha
Roll No: 07000006
Semester VII
B. Tech. Part IV

Alok Ranjan
Roll No: 07000005
Semester VII
B. Tech. Part IV

Mentored by
Rajeev Srivastava
Associate Professor
Department of Computer Engineering
Institute of Technology
Banaras Hindu University

CERTIFICATE

This is to certify that Abhinav Kumar Kushwaha (Roll no. 07000006) and Alok Ranjan (Roll no. 07000005 students of the Department of Computer Science& Engineering , Institute of Technology, Banaras Hindu University, Varanasi worked for his B.Tech. Major Project Phase – I entitled "Speckle reduction and segmentation in medical images*" under my supervision from beginning of seventh semester of B.Tech. program 2007-11.*

The report submitted by them embodies the literature from various reputed resources and is an authentic record of the work carried out by them under my supervision and guidance.

Rajeev Srivastava
Associate Professor
Department of Computer Engineering
IT-BHU

ACKNOWLEDGEMENT

It has been indeed a great privilege for us to have **Mr. Rajeev Srivastava** Associate Professor, Department of Computer Engineering, Institute of Technology, Banaras Hindu University, as our supervisor. His inspiring personality, superb guidance and constant encouragement are the motive force behind this project work. We take this opportunity to express our utmost gratitude to him.

We are highly grateful to Prof. **A. K. Agarwal**, Head, Department of Computer Engineering, Institute of technology, Banaras Hindu University for providing necessary facilities and encouragement during the course of work.

We are very thankful to all technical and non-technical staff of the Department of Computer Science & Engineering for their constant assistance and co-operation.

Abhinav Kumar Kushwaha
Roll No: 07000006
Semester VII
B. Tech. Part IV

Alok Ranjan
Roll No: 07000005
Semester VII
B. Tech. Part IV

Contents

Abstract

Speckle noise is a ubiquitous artifact that limits the interpretation of optical coherence tomography images and ultrasound images. Here we apply various speckle-reduction digital filters to OCT and US images and compare their performances. Our results indicate that adaptive filters, enhanced Lee, Frost and Wiener filters can significantly reduce speckle and increase the signal-to-noise ratio, while preserving strong edges.

In computer vision, segmentation refers to the process of partitioning a digital image into multiple segments (sets of pixels, also known as super pixels). The goal of segmentation is to simplify and/or change the representation of an image into something that is more meaningful and easier to analyze.

Here, we present a tool which can perform speckle reduction and segmentation both using several methods and then compare the results obtained.

KEYWORDS: Speckle Reduction, Medical Image, Image Segmentation, Ultrasound Image, Image Processing, SRAD filter, Lee Filter, Frost Filter, PDE based filter, Tool design, Performance Comparison.

1. Introduction

Medical imaging is the technique and process used to create images of the human body (or parts and function thereof) for clinical purposes (medical procedures seeking to reveal, diagnose or examine disease) or medical science (including the study of normal anatomy and physiology). Although imaging of removed organs and tissues can be performed for medical reasons, such procedures are not usually referred to as medical imaging, but rather are a part of pathology.

As a discipline and in its widest sense, it is part of biological imaging and incorporates radiology (in the wider sense), nuclear medicine, investigative radiological sciences, endoscopy, (medical) thermography, medical photography and microscopy (e.g. for human pathological investigations).

Measurement and recording techniques which are not primarily designed to produce images, such as electroencephalography (EEG), magnetoencephalography (MEG), Electrocardiography (EKG) and others, but which produce data susceptible to be represented as maps (i.e. containing positional information), can be seen as forms of medical imaging.

In the clinical context, "invisible light" medical imaging is generally equated to radiology or "clinical imaging" and the medical practitioner responsible for interpreting (and sometimes acquiring) the images is a radiologist. "Visible light" medical imaging involves digital video or still pictures that can be seen without special equipment. Dermatology and wound care are two modalities that utilize visible light imagery. Diagnostic radiography designates the technical aspects of medical imaging and in particular the acquisition of medical images. The *radiographer* or *radiologic technologist* is usually responsible for acquiring medical images of diagnostic quality, although some radiological interventions are performed by radiologists. While radiology is an evaluation of anatomy, nuclear medicine provides functional assessment.

As a field of scientific investigation, medical imaging constitutes a sub-discipline of biomedical engineering, medical physics or medicine depending on the context: Research and development in the area of instrumentation, image

acquisition (e.g. radiography), modelling and quantification are usually the preserve of biomedical engineering, medical physics and computer science; Research into the application and interpretation of medical images is usually the preserve of radiology and the medical sub-discipline relevant to medical condition or area of medical science (neuroscience, cardiology, psychiatry, psychology, etc.) under investigation. Many of the techniques developed for medical imaging also have scientific and industrial applications.

Medical imaging is often perceived to designate the set of techniques that noninvasively produce images of the internal aspect of the body. In this restricted sense, medical imaging can be seen as the solution of mathematical inverse problems. This means that cause (the properties of living tissue) is inferred from effect (the observed signal). In the case of ultrasonography the probe consists of ultrasonic pressure waves and echoes inside the tissue show the internal structure. In the case of projection radiography, the probe is X-ray radiation which is absorbed at different rates in different tissue types such as bone, muscle and fat.

The term noninvasive is a term based on the fact that following medical imaging modalities do not penetrate the skin physically. But on the electromagnetic and radiation level, they are quite invasive. From the high energy photons in X-Ray Computed Tomography, to the 2+ Tesla coils of an MRI device, these modalities alter the physical and chemical reactions of the body in order to obtain data.

As the requirement of medical image is so important, it is also very necessary to obtain such images clean and intact. Medical images get denoised due two speckle reduction because of which it becomes necessary to search for algorithms for better quality of images. In the field of medical, image with areas segmented is required. Here the implementation of algorithms for segmentation has also been done. In this report, we start from introduction and importance of medical images and then some details for image processing. Further we introduce ultrasound images and methods for speckle reduction and segmentation. We compare the results of speckle reduced images on parameters PSNR, peak signal-to-noise ratio and mean square error.

1.1 Image Processing

In electrical engineering and computer science, image processing is any form of signal processing for which the input is an image, such as a photograph or video frame; the output of image processing may be either an image or, a set of characteristics or parameters related to the image. Most image-processing techniques involve treating the image as a two-dimensional signal and applying standard signal-processing techniques to it.

Image processing usually refers to digital image processing, but optical and analog image processing also are possible. This article is about general techniques that apply to all of them. The acquisition of images (producing the input image in the first place) is referred to as imaging.

1.2 Typical Operations

* Euclidean geometry transformations such as enlargement, reduction, and rotation
* Color corrections such as brightness and contrast adjustments, color mapping, color balancing, quantization, or color translation to a different color space
* Digital compositing or optical compositing (combination of two or more images), which is used in film-making to make a "matte"
* Interpolation, demosaicing, and recovery of a full image from a raw image format using a Bayer filter pattern
* Image registration, the alignment of two or more images
* Image differencing and morphing
* Image recognition, for example, may extract the text from the image using optical character recognition or checkbox and bubble values using optical mark recognition
* Image segmentation
* High dynamic range imaging by combining multiple images
* Geometric hashing for 2-D object recognition with affine invariance

1.3 Ultrasound Image

Medical ultrasonography uses high frequency broadband sound waves in the megahertz range that are reflected by tissue to varying degrees to produce (up to 3D) images. This is commonly associated with imaging the fetus in pregnant women. Uses of ultrasound are much broader, however. Other important uses include imaging the abdominal organs, heart, breast, muscles, tendons, arteries

and veins. While it may provide less anatomical detail than techniques such as CT or MRI, it has several advantages which make it ideal in numerous situations, in particular that it studies the function of moving structures in real-time, emits no ionizing radiation, and contains speckle that can be used in elastography.

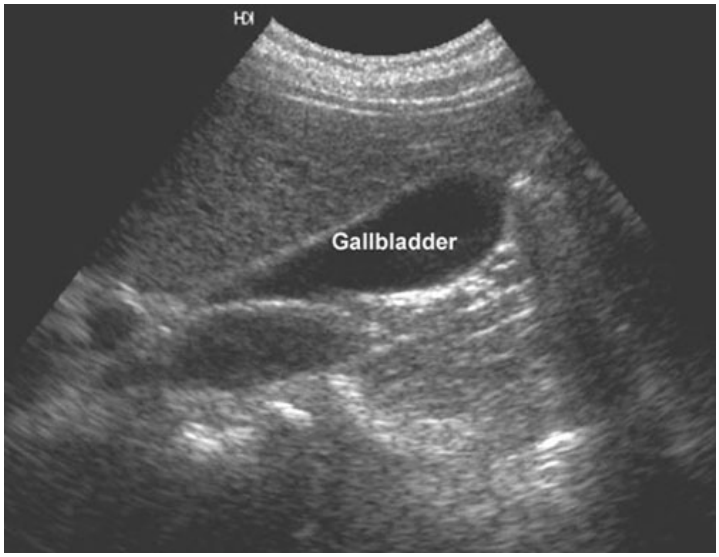

Ultrasound is also used as a popular research tool for capturing raw data, that can be made available through an Ultrasound research interface, for the purpose of tissue characterization and implementation of new image processing techniques. The concepts of ultrasound differ from other medical imaging modalities in the fact that it is operated by the transmission and receipt of sound waves. The high frequency sound waves are sent into the tissue and depending on the composition of the different tissues; the signal will be attenuated and returned at separate intervals. A path of reflected sound waves in a multilayered structure can be defined by an input acoustic impedance(Ultrasound sound wave) and the Reflection and transmission coefficients of the relative structures[3]. It is very safe to use and does not appear to cause any adverse effects, although information on this is not well documented. It is also relatively inexpensive and quick to perform. Ultrasound scanners can be taken to critically ill patients in intensive care units, avoiding the danger caused while moving the patient to the radiology department. The real time moving image obtained can be used to guide drainage and biopsy procedures. Doppler capabilities on modern scanners allow the blood flow in arteries and veins to be assessed.

1.4 Tomography

Tomography is the method of imaging a single plane, or slice, of an object resulting in a tomogram. There are several forms of tomography:

* Linear tomography: This is the most basic form of tomography. The X-ray tube moved from point "A" to point "B" above the patient, while the cassette holder (or "bucky") moves simultaneously under the patient from point "B" to point "A." The fulcrum, or pivot point, is set to the area of interest. In this manner, the points above and below the focal plane are blurred out, just as the background is blurred when panning a camera during exposure. No longer carried out and replaced by computed tomography.

* Poly tomography: This was a complex form of tomography. With this technique, a number of geometrical movements were programmed, such as hypocycloidic, circular, figure 8, and elliptical. Philips Medical Systems [1] produced one such device called the 'Polytome.' This unit was still in use into the 1990s, as its resulting images for small or difficult physiology, such as the inner ear, was still difficult to image with CTs at that time. As the resolution of CTs got better, this procedure was taken over by the CT.

* Zonography: This is a variant of linear tomography, where a limited arc of movement is used. It is still used in some centres for visualising the kidney during an intravenous urogram (IVU).

* Orthopantomography (OPT or OPG): The only common tomographic examination in use. This makes use of a complex movement to allow the radiographic examination of the mandible, as if it were a flat bone. It is often referred to as a "Panorex", but this is incorrect, as it is a trademark of a specific company.

* Computed Tomography (CT), or Computed Axial Tomography (CAT: A CT scan, also known as a CAT scan), is a helical tomography (latest generation), which traditionally produces a 2D image of the structures in a thin section of the body. It uses X-rays. It has a greater ionizing radiation dose burden than projection radiography; repeated scans must be limited to avoid health effects. CT is based on the same principles as X-Ray projections but in this case, the

patient is enclosed in a surrounding ring of detectors assigned with 500-1000 scintillation detectors[2]

. This being the fourth-generation X-Ray CT scanner geometry. Previously in older generation scanners, the X-Ray beam was paired by a translating source and detector.

1.5 Optical Coherence Tomography:

Optical coherence tomography (OCT) is an optical signal acquisition and processing method. It captures micrometer-resolution, three-dimensional images from within optical scattering media (e.g., biological tissue). Optical coherence tomography is an interferometric technique, typically employing near-infrared light. The use of relatively long wavelength light allows it to penetrate into the scattering medium.

Commercially available optical coherence tomography systems are employed in diverse applications, including art conservation and diagnostic medicine, notably in ophthalmology where it can be used to obtain detailed images from within the retina.

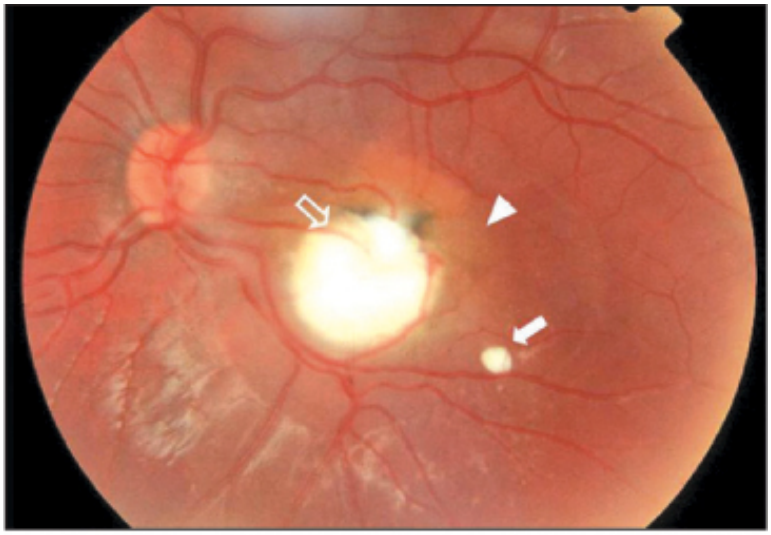

Figure 1 - Fundus photograph of the posterior pole of the left eye shows a large whitish elevated lesion (open arrow) with an ill-defined yellowish temporal border (arrowhead) associated with a smaller satellite lesion (arrow). Pigment hypertrophy and surrounding subretinal fluid were observed.

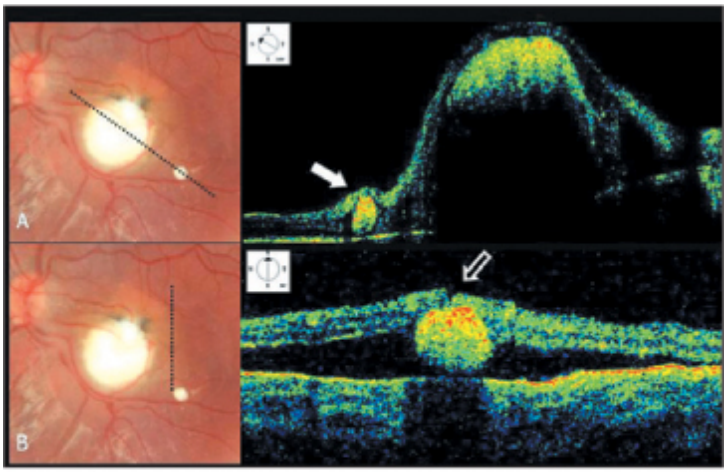

Figure 2 - A: OCT scan reveals an elevated large subretinal lesion with serous retinal detachment associated with a smaller satellite lesion (arrow); B: OCT shows in a macular vertical scan a highly reflective subfoveal spherical mass protruding above the retinal pigment epithelium with posterior shadow and surrounding subretinal fluid (open arrow).

1.6 Use in pharmaceutical clinical trials

Medical imaging has become a major tool in clinical trials since it enables rapid diagnosis with visualization and quantitative assessment.

A typical clinical trial goes through multiple phases and can take up to eight years. Clinical endpoints or outcomes are used to determine whether the therapy is safe and effective. Once a patient reaches the endpoint, he/she is generally excluded from further experimental interaction. Trials that rely solely on clinical endpoints are very costly as they have long durations and tend to need large number of patients.

In contrast to clinical endpoints, surrogate endpoints have been shown to cut down the time required to confirm whether a drug has clinical benefits. Imaging biomarkers (a characteristic that is objectively measured by an imaging technique, which is used as an indicator of pharmacological response to a therapy) and surrogate endpoints have shown to facilitate the use of small group sizes, obtaining quick results with good statistical power.[8]

Imaging is able to reveal subtle change that is indicative of the progression of therapy that may be missed out by more subjective, traditional approaches. Statistical bias is reduced as the findings are evaluated without any direct patient contact.

For example, measurement of tumour shrinkage is a commonly used surrogate endpoint in solid tumour response evaluation. This allows for faster and more objective assessment of the effects of anticancer drugs. In evaluating the extent of Alzheimer's disease, it is still prevalent to use behavioural and cognitive tests. MRI scans on the entire brain can accurately pinpoint hippocampal atrophy rate while PET scans is able to measure the brain's metabolic activity by measuring regional glucose metabolism.[8]

An imaging-based trial will usually be made up of three components:

1. A realistic imaging protocol. The protocol is an outline that standardizes (as far as practically possible) the way in which the images are acquired using the various modalities (PET, SPECT, CT, MRI). It covers the specifics in which images are to be stored, processed and evaluated.

2. An imaging centre that is responsible for collecting the images, perform quality control and provide tools for data storage, distribution and analysis. It is important for images acquired at different time points are displayed in a standardised format to maintain the reliability of the evaluation. Certain specialised imaging contract research organizations provide to end medical imaging services, from protocol design and site management through to data quality assurance and image analysis.

3. Clinical sites that recruit patients to generate the images to send back to the imaging centre.

2. Speckle Pattern and Segmentation

2.1 Speckle Pattern

A **speckle pattern** is a random intensity pattern produced by the mutual interference of a set of wavefronts. This phenomenon has been investigated by scientists since the time of Newton, but speckles have come into prominence since the invention of the laser and have now found a variety of applications.

The speckle effect is a result of the interference of many waves, having different phases, which add together to give a resultant wave whose amplitude, and therefore intensity, varies randomly. If each wave is modelled by a vector, then it can be seen that if a number of vectors with random angles are added together, the length of the resulting vector can be anything from zero to the sum of the individual vector lengths—a 2-dimensional random walk, sometimes known as a drunkard's walk.

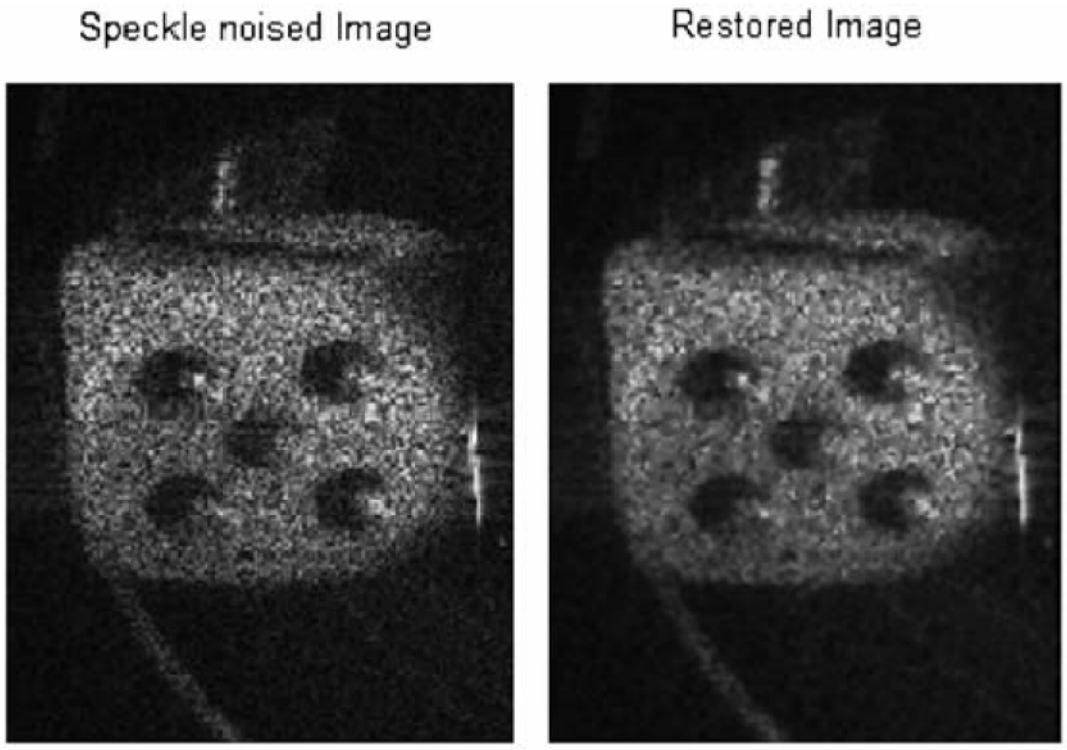

When a surface is illuminated by a light wave, according to diffraction theory, each point on an illuminated surface acts as a source of secondary spherical waves. The light at any point in the scattered light field is made up of waves which have been scattered from each point on the illuminated surface. If the

surface is rough enough to create path-length differences exceeding one wavelength, giving rise to phase changes greater than 2π, the amplitude, and hence the intensity, of the resultant light varies randomly.

If light of low coherence (i.e. made up of many wavelengths) is used, a speckle pattern will not normally be observed, because the speckle patterns produced by individual wavelengths have different dimensions and will normally average one another out. However, speckle patterns can be observed in polychromatic light in some conditions.

2.1.1 Application

When lasers were first invented, the speckle effect was considered to be a severe drawback in using lasers to illuminate objects, particularly in holographic imaging because of the grainy image produced. It was later realized that speckle patterns could carry information about the object's surface deformations, and this effect is exploited in holographic interferometry and electronic speckle pattern interferometry. The speckle effect is also used in stellar speckle astronomy, speckle imaging and in eye testing using speckle.

Speckle is the chief limitation of coherent imaging in optical heterodyne detection.

In the case of near field speckles, the statistical properties depend on the light scattering distribution of a given sample. This allows to use the near field speckles analysis as a way to detect the scattering distribution; this is the so-called near-field scattering technique.

2.1.2 Speckle Reducing Techniques:

The successful removal of this artifact is therefore considered to be essential if the full potential of medical ultrasound imaging is to be realized. It should be noted that the acceptability of a speckle correction procedure (for medical images) will be greatly increased if it can be implemented on a real-time basis.

A number of techniques are available for processing the bad scattered signal in attempting to remove the speckle artifact before display. Speckle reduction methods fall broadly into three categories and these are outlined below.

- **Filtering Techniques:**

  Filtering techniques for removing the speckle artifact involve processing of the entire image - either in one step, or via partitioning into a number of sub-images - and therefore result in modification of regions not significantly affected by the artifact. Adaptive filtering techniques, which process each image partition differently, according to the degree of speckle present, are an improvement, but rely on a statistical identification of speckle.
  We have implemented these techniques in our tool.

- **Spatial or Frequency Compounding:**

  The second class covers methods that implement spatial or frequency compounding. The former entails combining a number of images taken from different angles of view. These are then compounded by some *ad hoc* procedure in the hope that the apparently noise-like speckle pattern will be averaged to a low level, compared to the more stable image features that correspond to true tissue structure. One difficulty (amongst many) is that it is applicable to only a few sites of clinical interest. Frequency compounding involves averaging pulse-echo images produced using pulses with differing centre frequencies. The 'frequency diversity' method applies (minimally overlapping) narrow bandpass filters to split the received signal into separate imaging channels**.** Each channel is then usually envelope detected, and all the channels compounded by some method. Gehlbach suggests that coherent compounding (i.e. without envelope detection) may be sufficient, thereby reducing the process to a single filter.

  In common with filtering techniques, the frequency compounding methods also result in modification of image regions not affected by the speckle artifact, and hence some loss of available informational content. However**,** since frequency diversity is applied to individual A-lines, this implies the feasibility of a real-time implementation. The method may be useful where spatial resolution can be sacrificed for contrast resolution.

- **Phase Acknowledging Techniques:**

The third class of speckle reduction procedures attempts to utilize this information for recognition (stage 1) and/or correction (stage 2) and will be referred to as **phase acknowledging techniques**. Large excursions in instantaneous frequency from the carrier frequency of the imaging pulse can be used to deterministically identify regions of speckle corruption.
Hence consideration of temporal phase can demarcate local speckle corrupted segments (stage 1). A number of methods take advantage of this localization property for correction, namely local frequency diversity techniques.

2.2 Segmentation

In computer vision, segmentation refers to the process of partitioning a digital image into multiple segments (sets of pixels, also known as superpixels). The goal of segmentation is to simplify and/or change the representation of an image into something that is more meaningful and easier to analyze.[4] Image segmentation is typically used to locate objects and boundaries (lines, curves, etc.) in images. More precisely, image segmentation is the process of assigning a label to every pixel in an image such that pixels with the same label share certain visual characteristics.

(a) Color Labels (ACA) (b) Texture Classes

(c) Crude Segmentation (d) Final Segmentation

The result of image segmentation is a set of segments that collectively cover the entire image, or a set of contours extracted from the image (see edge detection). Each of the pixels in a region are similar with respect to some characteristic or computed property, such as color, intensity, or texture. Adjacent regions are significantly different with respect to the same characteristic(s).[4]

2.2.1 Clustering Method

The K-means algorithm is an iterative technique that is used to partition an image into K clusters. The basic algorithm is:

1. Pick K cluster centers, either randomly or based on some heuristic
2. Assign each pixel in the image to the cluster that minimizes the distance between the pixel and the cluster center
3. Re-compute the cluster centers by averaging all of the pixels in the cluster
4. Repeat steps 2 and 3 until convergence is attained (e.g. no pixels change clusters)

In this case, distance is the squared or absolute difference between a pixel and a cluster center. The difference is typically based on pixel color, intensity, texture, and location, or a weighted combination of these factors. K can be selected manually, randomly, or by a heuristic.

This algorithm is guaranteed to converge, but it may not return the optimal solution. The quality of the solution depends on the initial set of clusters and the value of K.

In statistics and machine learning, the k-means algorithm is clustering algorithm to partition n objects into k clusters, where k < n. It is similar to the expectation-maximization algorithm for mixtures of Gaussians in that they both attempt to find the centers of natural clusters in the data. The model requires that the object attributes correspond to elements of a vector space. The objective it tries to achieve is to minimize total intra-cluster variance, or, the squared error function. The k-means clustering was invented in 1956. The most common form of the algorithm uses an iterative refinement heuristic known as Lloyd's algorithm. Lloyd's algorithm starts by

partitioning the input points into k initial sets, either at random or using some heuristic data. It then calculates the mean point, or centroid, of each set. It constructs a new partition by associating each point with the closest centroid. Then the centroids are recalculated for the new clusters, and algorithm repeated by alternate application of these two steps until convergence, which is obtained when the points no longer switch clusters (or alternatively centroids are no longer changed). Lloyd's algorithm and k-means are often used synonymously, but in reality Lloyd's algorithm is a heuristic for solving the k-means problem, as with certain combinations of starting points and centroids, Lloyd's algorithm can in fact converge to the wrong answer. Other variations exist, but Lloyd's algorithm has remained popular, because it converges extremely quickly in practice. In terms of performance the algorithm is not guaranteed to return a global optimum. The quality of the final solution depends largely on the initial set of clusters, and may, in practice, be much poorer than the global optimum. Since the algorithm is extremely fast, a common method is to run the algorithm several times and return the best clustering found. A drawback of the k-means algorithm is that the number of clusters k is an input parameter. An inappropriate choice of k may yield poor results. The algorithm also assumes that the variance is an appropriate measure of cluster scatter.

2.2.2 Compression Based Method

Compression based methods postulate that the optimal segmentation is the one that minimizes, over all possible segmentations, the coding length of the data [3] [4]. The connection between these two concepts is that segmentation tries to find patterns in an image and any regularity in the image can be used to compress it. The method describes each segment by its texture and boundary shape. Each of these components is modeled by a probability distribution function and its coding length is computed as follows:

1. The boundary encoding leverages the fact that regions in natural images tend to have a smooth contour. This prior is used by huffman coding to encode the difference chain code of the contours in an image. Thus, the smoother a boundary is, the shorter coding length it attains.

2. Texture is encoded by lossy compression in a way similar to minimum description length (MDL) principle, but here the length of the data given the model is approximated by the number of samples times the entropy of the model. The texture in each region is modeled by a multivariate normal distribution whose entropy has closed form expression. An interesting property of this model is that the estimated entropy bounds the true entropy of the data from above. This is because among all distributions with a given mean and covariance, normal distribution has the largest entropy. Thus, the true coding length cannot be more than what the algorithm tries to minimize.

For any given segmentation of an image, this scheme yields the number of bits required to encode that image based on the given segmentation. Thus, among all possible segmentations of an image, the goal is to find the segmentation which produces the shortest coding length. This can be achieved by a simple agglomerative clustering method. The distortion in the lossy compression determines the coarseness of the segmentation and its optimal value may differ for each image. This parameter can be estimated heuristically from the contrast of textures in an image. For example, when the textures in an image are similar, such as in camouflage images, stronger sensitivity and thus lower quantization is required.

2.2.3 Histogram-Based Method

Histogram-based methods are very efficient when compared to other image segmentation methods because they typically require only one pass through the pixels. In this technique, a histogram is computed from all of the pixels in the image, and the peaks and valleys in the histogram are used to locate the clusters in the image.[1] Color or intensity can be used as the measure.

A refinement of this technique is to recursively apply the histogram-seeking method to clusters in the image in order to divide them into smaller clusters. This is repeated with smaller and smaller clusters until no more clusters are formed.[5]

One disadvantage of the histogram-seeking method is that it may be difficult to identify significant peaks and valleys in the image. In this technique of image classification distance metric and integrated region matching are familiar.

Histogram-based approaches can also be quickly adapted to occur over multiple frames, while maintaining their single pass efficiency. The histogram can be done in multiple fashions when multiple frames are considered. The same approach that is taken with one frame can be applied to multiple, and after the results are merged, peaks and valleys that were previously difficult to identify are more likely to be distinguishable. The histogram can also be applied on a per pixel basis where the information results are used to determine the most frequent color for the pixel location. This approach is segments based on active objects and a static environment, resulting in a different type of segmentation useful in Video tracking.

2.2.4 Partial Differential Equation based methods

Curve propagation is a popular technique in image analysis for object extraction, object tracking, stereo reconstruction, etc. The central idea behind such an approach is to evolve a curve towards the lowest potential of a cost function, where its definition reflects the task to be addressed and imposes certain smoothness constraints. Lagrangian techniques are based on parameterizing the contour according to some sampling strategy and then evolve each element according to image and internal terms. While such a technique can be very efficient, it suffers from various limitations like deciding on the sampling strategy, estimating the internal geometric properties of the curve, changing its topology, addressing problems in higher dimensions, etc. In each case, a partial differential equation (PDE) called the level set equation is solved by finite differences.

The level set method was initially proposed to track moving interfaces by Osher and Sethian in 1988 and has spread across various imaging domains in the late nineties. It can be used to efficiently address the problem of curve/surface/etc. propagation in an implicit manner. The central idea is to represent the evolving contour using a signed function, where its zero level

corresponds to the actual contour. Then, according to the motion equation of the contour, one can easily derive a similar flow for the implicit surface that when applied to the zero-level will reflect the propagation of the contour. The level set method encodes numerous advantages: it is implicit, parameter free, provides a direct way to estimate the geometric properties of the evolving structure, can change the topology and is intrinsic. Furthermore, they can be used to define an optimization framework as proposed by Zhao, Merriman and Osher in 1996. Therefore, one can conclude that it is a very convenient framework to address numerous applications of computer vision and medical image analysis.[6] Furthermore, research into various level set data structures has led to very efficient implementations of this method.

2.2.5 Graph Partitioning Methods

Graph partitioning methods can effectively be used for image segmentation. In these methods, the image is modeled as a weighted, undirected graph. Usually a pixel or a group of pixels are associated with nodes and edge weights define the (dis)similarity between the neighborhood pixels. The graph (image) is then partitioned according to a criterion designed to model "good" clusters. Each partition of the nodes (pixels) output from these algorithms are considered an object segment in the image. Some popular algorithms of this category are normalized cuts [7], random walker [8], minimum cut [9], isoperimetric partitioning [10] and minimum spanning tree-based segmentation [11].

2.2.6 Watershed Transformation

The watershed transformation considers the gradient magnitude of an image as a topographic surface. Pixels having the highest gradient magnitude intensities (GMIs) correspond to watershed lines, which represent the region boundaries. Water placed on any pixel enclosed by a common watershed line flows downhill to a common local intensity minimum (LIM). Pixels draining to a common minimum form a catch basin, which represents a segment.

2.3 Work Done in this field

1. **MIPAV**
   Introduction

   The MIPAV (Medical Image Processing, Analysis, and Visualization) application enables quantitative analysis and visualization of medical images of numerous modalities such as PET, MRI, CT, or microscopy. Using MIPAV's standard user-interface and analysis tools, researchers at remote sites (via the internet) can easily share research data and analyses, thereby enhancing their ability to research, diagnose, monitor, and treat medical disorders.

   MIPAV is a Java application and can be run on any Java-enabled platform such as Windows, UNIX, or Macintosh OS X.

   Goals for MIPAV

   MIPAV is to meet the following goals:

   - To develop computational methods and algorithms to analyze and quantify biomedical data;
   - To collaborate with NIH researchers and colleagues at other research centers in applying information analysis and visualization to biomedical research problems;
   - To develop tools (in both hardware and software) to give our collaborators the ability to analyze biomedical data to support the discovery and advancement of biomedical knowledge.

   Need for MIPAV

   Imaging has become an essential component in many fields of bio-medical research and clinical practice. Biologists study cells and generate 3D confocal microscopy data sets, virologists generate 3D reconstructions of viruses from micrographs, radiologists identify and quantify tumors from MRI and CT scans, and neuroscientists detect regional metabolic brain activity from PET and functional MRI scans. Analysis of these diverse types of images requires sophisticated computerized quantification and visualization tools. To support scientific research in the NIH intramural

program, CIT has made major progress in the development of a platform-independent, n-dimensional, general-purpose, extensible image processing and visualization program.

2. In the paper[12] published by Joachim Weickert, the goal of paper is to investigate segmentation methods that combine fast preprocessing algorithms using partial differential equations (PDEs) with a watershed transformation with region merging. We consider two well-founded PDE methods: a nonlinear isotropic di!usion "lter that permits edge enhancement, and a convex quadratic variational image restoration method which gives good denoising. For the di!usion "lter, an e$cient algorithm is applied using an additive operator splitting (AOS) that leads to recursive and separable "lters. For the variational restoration method, a novel algorithm is developed that uses AOS schemes within a Gaussian pyramid decomposition. Examples demonstrate that preprocessing by these PDE techniques signi"cantly improves the watershed segmentation, and that the resulting segmentation method gives better results than some traditional techniques. The algorithm has linear complexity and it can be used for arbitrary dimensional data sets.

3. In the paper[13] published by Anastasia Sofou and Petros Maragos, the classical case of morphological segmentation is based on the watershed transform, constructed by flooding the gradient image, which is seen as a topographic surface, with constant height speed. Changing the flooding criteria, (e.g constant-speed height, area or volume) yields different segmentation results. In the field of PDEs and curve evolution the classic watershed transform can be modelled as the solution of an eikonal PDE. In this paper we model the watershed segmentation based on a volume flooding criterion via a different eikonal PDE. Then we solve this PDE using the fast marching method, which is a specific algorithm from the methodology of level sets. In addition, we attempt to exploit the advantages of image segmentation using PDE-based volume looding over the classic height flooding.

4. In this paper[14] published by Rajeev Srivastav, JRP Gupta and Harish Parthaswamy, the partial differential equation (PDE) based homomorphic filtering technique is proposed for speckle reduction from digitally reconstructed holographic images based on the concepts of complex diffusion processes. For digital implementations, the proposed scheme was discretized using finite differences scheme.Further,the performance of the proposed PDE-based technique is compared with other speckle reduction techniques such as homomorphic anisotropic diffusion filter based on extended concept of Perona and Malik(1990) [2], homomorphic Weiner filter, Lee filter, Frost filter, Kuan filter, speckle reducing an isotropic diffusion(SRAD) filter and hybrid filter in the context of digital holography. For the comparison of various speckle reduction techniques,the performance is evaluated quantitatively in terms of all possible parameters that justify the applicability of a scheme for a specific application. The chosen parameters are mean-square-error(MSE), normalized mean-square-error(NMSE), peak signal-to-noiseratio(PSNR), speckleindex, average signal-to-noise ratio(SNR), effective number of looks(ENL), correlation parameter(CP), mean structure similarity index map(MSSIM) and execution time in seconds.For experimentation and computer simulation MATLAB7. 0has been used and the performance is evaluated and tested for various sample holographic images for varying amount of speckle variance.The results obtained justify the applicability of proposed schemes.

3. Speckle Reduction

The **Filtering Approaches for Speckle Reduction** used in our tool are:

1. **SRAD (Speckle Reducing Anisotropic Diffusion)**
2. **Frost Filter**
3. **Lee Filter**
4. **PDE based homomorphic filtering for speckle reduction**

3.1 SRAD (Speckle Reducing Anisotropic Diffusion)

It is a partial differential equation (PDE) approach to speckle removal that we call speckle reducing anisotropic diffusion (SRAD). The PDE-based speckle removal approach allows the generation of an image scale space (a set of filtered images that vary from fine to coarse) without bias due to filter window size and shape.

SRAD not only preserves edges but also enhances edges by inhibiting diffusion across edges and allowing diffusion on either side of the edge. SRAD is adaptive and does not utilize hard thresholds to alter performance in homogeneous regions or in regions near edges and small features.

The new diffusion technique is based on the same minimum mean square error (MMSE) approach to filtering as the Lee, Kuan and Frost filters. In fact, we show that the SRAD can be related directly to the Lee and Frost window-based filters. So, SRAD is the edge sensitive extension of conventional adaptive speckle filter, in the same manner that the original Perona and Malik anisotropic diffusion is the edge sensitive extension of the average filter.

In this sense, we extend the application of anisotropic diffusion to applications such as OCT and medical ultrasound in which signal-dependent, spatially correlated multiplicative noise is present.

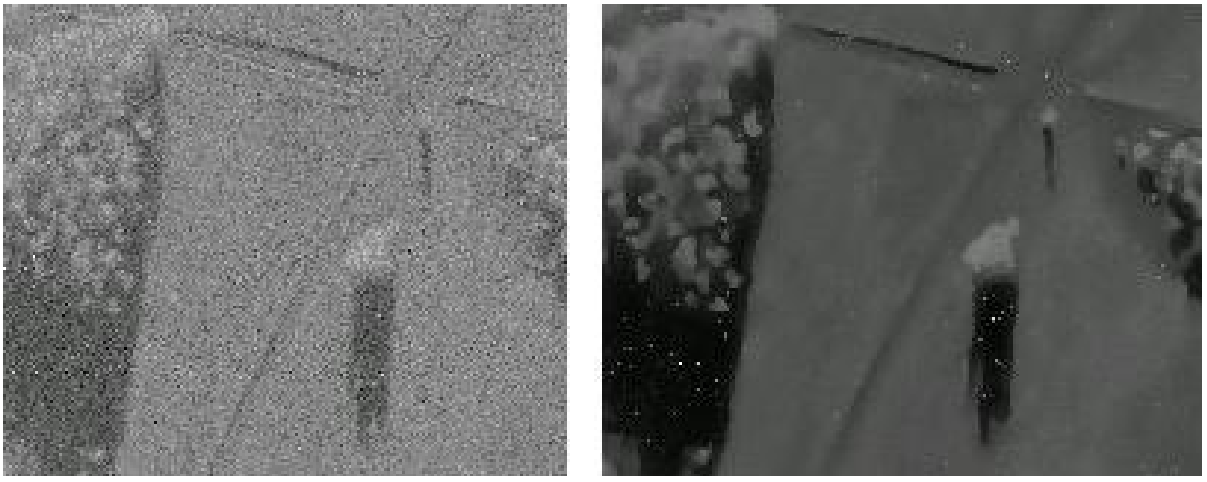

Radar image of Battle Field (left) and the image after SRAD filter (right)

Here is source code for srad filter where input is a noisy image and output is filtered image.

Source Code (SRAD):

```
% Input :  I- noisy image
% Output: S – filtered image

function S=srad(I)
tic
T=10;
[x y]=size(I);
I=double(I);
Ic=double(I);
delta_t = 0.08;
t=1;
eps=0.00000000001;
for t=1:T
   qt=exp(-t*.2);
   [Ix,Iy] = gradient(Ic);
   di=sqrt(Ix.^2+Iy.^2);
   di2=del2(Ic);
   T1=0.5*((di./(Ic+eps)).^2);
   T2=0.0625*((di2./(Ic+eps)).^2);
   T3=(1+(0.25*(di2./(Ic+eps)))).^2;
   T=sqrt((T1-T2)./(T3+eps));
   dd=(T.^2-qt.^2)./((qt.^2*(1+qt.^2)+eps));
   cq=1./(1+dd);
   [D1,D2]=gradient(cq.*Ix);
   [D3,D4]=gradient(cq.*Iy);
   D=D1+D4;
   Ic=real(Ic+delta_t .*D);
end
toc
S=uint8(Ic);
imwrite(S,'srad.jpg');
```

3.2 Frost Filter

FROST is used primarily to filter speckled SAR data. An adaptive Frost filter smoothes image data, without removing edges or sharp features in the images.

Frost filter algorithm is an exponentially damped convolution kernel which adapts itself to features by using local statistics. The adaptive filter computes a set of weight values for each pixel within the filter window surrounding each pixel.

The Frost filter differs from the Lee and Kuan filters with respect that the scene reflectivity is estimated by convolving the observed image with the impulse response of the SAR system. The impulse response of the SAR system is obtained by minimizing the mean square error between the observed image and the scene reflectivity model which is assumed to be an autoregressive process.

The damping factor for adaptive filtering (DAMP) depends on the non-filtered image and may require trial-and-error experiments to determine the best value. The value of DAMP defines the extent of the exponential damping (the smaller the value, the smaller the damping effect). The default value for DAMP is 1.

The MASK parameter specifies the area within the input channel which will be processed. Only the area under the mask will be filtered, and the rest of the image will be unchanged. If a single value is specified, then this value points to a bitmap segment, which define the area to be filtered. When four values are specified, these values define the x,y offsets and x,y dimensions of rectangular window within the image to be filtered. If defaulted, the entire database is processed.

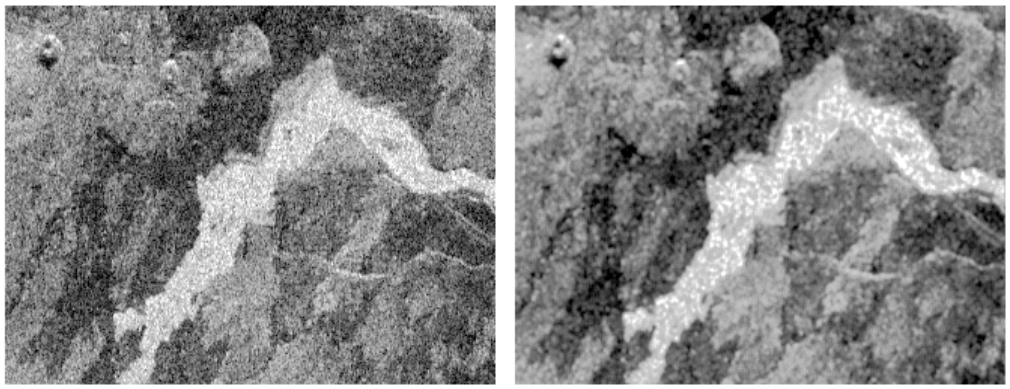

Radar image (left) and its Frost filtered image (right)

Algorithm:

1. Centre the filter window on the target pixel.
2. Calculate y(t) using A, B, and C.
3. Replace the value of the target pixel with the value y(t).
4. Go to the first step until the whole image is processed.

$$\text{A)} \quad a^2 = s^2 / z^2$$

$$\text{B)} \quad m(t) = e^{-Ka^2|t|}$$

$$\text{C)} \quad y(t) = \frac{\sum_i [m(t_i)x(t_i)]}{\sum_i [m(t_i)]}$$

- s^2 : Image variance
- z : Image mean
- t : Pixel coordinate
- m(t) : Weight factor
- K : Constant
- x(t) : Original pixel value in the point t.
- y(t) : Replacing pixel value for the point t.

Here is source code for frost filter where input is a noisy image and output is filtered image.

Source Code (Frost):

```
% Input: I - noisy image
% Output : ft - filtered image
function [ft]=frost(I)
tic
[x y z]=size(I);
I=double(I);
K=1;
```

```
N=I;
for i=1:x
    for j=1:y
        if (i>1 & i<x & j>1 & j<y)
            mat(1)=I(i-1,j);
            mat(2)=I(i+1,j);
            mat(3)=I(i,j-1);
            mat(4)=I(i,j+1);
            d(1)=sqrt((i-(i-1))^2);
            d(2)=sqrt((i-(i+1))^2);
            d(3)=sqrt((j-(j-1))^2);
            d(4)=sqrt((j-(j+1))^2);
            mn=mean(mean(mat));
            c=mat-mn;
            c2=c.^2;
            c3=c/(c2+.0000001);
            Cs=0.25*sum(sum(c3));
            m(1)=exp(-K*Cs*d(1));
            m(2)=exp(-K*Cs*d(2));
            m(3)=exp(-K*Cs*d(3));
            m(4)=exp(-K*Cs*d(4));
            ms=sum(sum(m));
            mp=m/ms;
            N(i,j)=sum(sum(mp.*mat));
        end
     end
end
toc
ft=uint8(N);
imwrite(ft,'frost2.jpg');
```

3.3 Lee Filter

The Lee filter uses a least-squares approach to estimate the true signal strength of the center cell in the filter window from the measured value in that cell, the local mean brightness of all cells in the window, and a gain factor calculated from the local variance and the noise standard deviation.
The filter assumes a Gaussian (normal) distribution for the noise values, and calculates the local noise standard deviation for each filter window.

The Lee filter calculation produces an output value close to the local mean for uniform areas, and a value close to the original input value in higher contrast regions. Most smoothing occurs in the more uniform areas, while edges and other fine detail is maintained. The Lee filter has no user-defined parameters.

A bitmap specifies the area within the input layer which will be processed. Only this area will be filtered and the rest of the image will be unchanged. If no bitmap is connected, the entire database is processed.

The Lee filter model requires that the signal represents power. If the input image is in amplitude format, each grey level will be squared to derive power and finally square root will be applied to the filtered result.

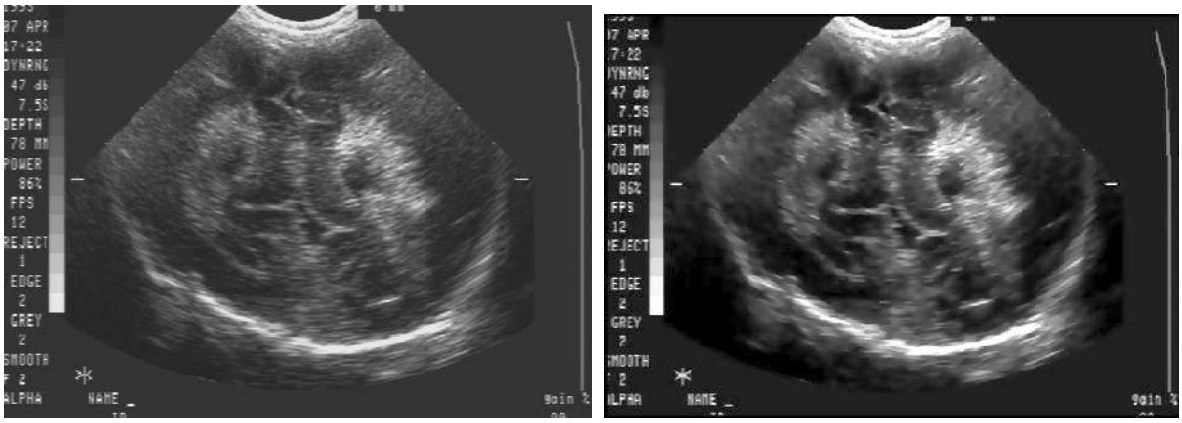

Original Ultrasound image (left) and Lee filtered image (right)

Algorithm:

Speckle noise in SAR images is generally assumed a multiplicative error model. In the Lee filter, the multiplicative model is first approximated by a linear model. Then the minimum mean square error criterion is applied to the linear model. The resulting grey level value R for the smoothed pixel is:

R = Ic * W + Im * (1 - W)

where:

W = 1 - Cu^2/Ci^2
Cu = SQRT(1/NLOOK)
Ci = S / Im
Ic = center pixel pixel of filter window
Im = mean value of intensity within window
S = standard deviation of intensity within window

The Cu above is the estimated noise variation coefficient. Ci is the image variation coefficient. W is a weighting function.

Here is source code for lee filter where input is a noisy image and output is filtered image.

Source Code:

```
% Input : I – noisy image
% Output: le – filtered image

function [le]=lee()
I=imread('3.jpg');
[x y z]=size(I)
I=double(I);
N=zeros(x,y,z);
for i=1:x
    i
    for j=1:y
        % Checking first and last pixel of first row%
        if (i==1 & j==1)
            mat(1)=0;
            mat(2)=0;
            mat(3)=0;
            mat(4)=0;
            mat(5)=I(i,j);
            mat(6)=I(i,j+1);
```

```
    mat(7)=0;
    mat(8)=I(i+1,j);
    mat(9)=I(i+1,j+1);
end

if (i==1 & j==y)
    mat(1)=0;
    mat(2)=0;
    mat(3)=0;
    mat(4)=I(i,j-1);
    mat(5)=I(i,j);
    mat(6)=0;
    mat(7)=I(i+1,j-1);
    mat(8)=I(i+1,j);
    mat(9)=0;
end

% Checking first and last pixel of last row%
if (i==x & j==1)
    mat(1)=0;
    mat(2)=I(i-1,j);
    mat(3)=I(i-1,j+1);
    mat(4)=0;
    mat(5)=I(i,j);
    mat(6)=I(i,j+1);
    mat(7)=0;
    mat(8)=0;
    mat(9)=0;
end

if (i==x & j==y)
    mat(1)=I(i-1,j-1);
    mat(2)=I(i-1,j);
    mat(3)=0;
    mat(4)=I(i,j-1);
    mat(5)=I(i,j);
    mat(6)=0;
    mat(7)=0;
    mat(8)=0;
    mat(9)=0;
end
% Checking rest of the image%
if (i>1 & i<x & j>1 & j<y)
    mat(1)=I(i-1,j-1);
    mat(2)=I(i-1,j);
    mat(3)=I(i-1,j+1);
    mat(4)=I(i,j-1);
```

```
            mat(5)=I(i,j);
            mat(6)=I(i,j+1);
            mat(7)=I(i+1,j-1);
            mat(8)=I(i+1,j);
            mat(9)=I(i+1,j+1);
        end
        y1=I(i,j);
        ybar=mean(mean(mat));
        if ybar~=0
            ystad=std2(mat);
            ENL=(ybar/ystad)^2;
            sx2=((ENL*(ystad)^2)-(ybar)^2)/(ENL+1);
            xcap=ybar+(sx2*(y1-ybar)/(sx2+(ybar^2/ENL)));
            N(i,j)=xcap;
        else
            N(i,j)=y1;
        end
    end
end
le=uint8(N);
imwrite(le,'lee2.jpg');
```

3.4 PDE based homomorphic filtering for speckle reduction

In PDE-based noise removal techniques [18], suppose I is a2D scalar noisy image that we want to restore and the noise can be considered as high-frequency variations with low amplitude, added to the pixels of the regular image.

$I_{noisy}=I_{regular}+\sigma$

Here, we consider PDE based anisotropic diffusion filter. This filter based filter has been successfully applied for removal of additive noise and enhancement of gray images. In anisotropic diffusion-based filter [2], the basic idea is that heat equation (13) for linear diffusion can be written in divergence form:

$\partial I/\partial t = \nabla^2 I = div(grad I) = \nabla.\nabla I$

The introduction of a conductivity coefficient c in the above diffusion equation makes it possible to make the diffusion adaptive to local image structure [2].

$\partial I/\partial t = \vec{\nabla}. c\vec{\nabla} I$

The two possible choices for diffusion constant c are :

$C_1 = exp(-\frac{||\nabla I||}{k^2})$ and $C_2 = \frac{1}{1+\frac{||\nabla I||^2}{k^2}}$ where k>0.

Both expressions are equal upto first-order approximation and k is a fixed gradient threshold that differentiates homogeneous area and regions of contours and edges. For digital implementation we can write the discretized form of finite difference scheme as

$I^{n+1}(x,y) = I^n(x,y) + \Delta t\ .\ (\vec{\nabla}. c\vec{\nabla} I)$

For the numerical scheme in the above equation to be stable, the von Neumann analysis shows that we require $\Delta t/(\Delta x)^2 < 0.25$. If the grid size is set to $\Delta x=1$, then $\Delta t<0.25$.

Here is source code for srad filter where input is a noisy image and output is filtered image.

Source Code:

```
% Input : I - noisy image
% output: P - filtered image

function P=pde_noise_reduction(I)
[x y]=size(I);
I=double(I);
I2=I;

T=7;
for t=1:T
    [Ix,Iy]=gradient(I);
    %c = 1./(1.+(Ix.^2+Iy.^2));
    c=exp((-1).*(sqrt(Ix.^2+Iy.^2))./7000);
    [div1,divt1]=gradient(c.*Ix);
    [divt2,div2]=gradient(c.*Iy);
    div=div1+div2;
    I1=I+(0.20).*div;
    I=I1;
end;
I=I2-I1;
S=uint8(I1);
imwrite(S,'pde.jpg');
S=uint8(I);
imwrite(S,'diff.jpg');
```

4. Image Segmentation

Segmentation refers to the process of partitioning a digital image into multiple segments. The goal of segmentation is to simplify and/or change the representation of an image into something that is more meaningful and easier to analyze. Image segmentation is typically used to locate objects and boundaries in images. More precisely, image segmentation is the process of assigning a label to every pixel in an image such that pixels with the same label share certain visual characteristics.

The result of image segmentation is a set of segments that collectively cover the entire image, or a set of contours extracted from the image. Each of the pixels in a region is similar with respect to some characteristic or computed property, such as color, intensity, or texture. Adjacent regions are significantly different with respect to the same characteristic(s).

Several general-purpose algorithms and techniques have been developed for image segmentation. Since there is no general solution to the image segmentation problem, these techniques often have to be combined with domain knowledge in order to effectively solve an image segmentation problem for a problem domain.

4.1 Thresholding

Thresholding is the simplest method of image segmentation. From a grayscale image, thresholding can be used to create binary images.

During the thresholding process, individual pixels in an image are marked as “object” pixels if their value is greater than some threshold value (assuming an object to be brighter than the background) and as “background” pixels otherwise. This convention is known as threshold above. Variants include threshold below, which is opposite of threshold above; threshold inside, where a pixel is labeled "object" if its value is between two thresholds; and threshold outside, which is the opposite of threshold inside. Typically, an object pixel is given a value of “1” while a background pixel is given a value of “0.” Finally, a binary image is created by coloring each pixel white or black, depending on a pixel's label.

4.2 Iterative Method

One method that is relatively simple, does not require much specific knowledge of the image, and is robust against image noise, is the following iterative method:

1. An initial threshold (T) is chosen, this can be done randomly or according to any other method desired.
2. The image is segmented into object and background pixels as described above, creating two sets:
    1. G1 = {f(m,n):f(m,n)>T} (object pixels)
    2. G2 = {f(m,n):f(m,n)\leT} (background pixels) (note, f(m,n) is the value of the pixel located in the mth column, nth row)
3. The average of each set is computed.
    1. m1 = average value of G1
    2. m2 = average value of G2
4. A new threshold is created that is the average of m1 and m2
    1. T' = (m1 + m2)/2
5. Go back to step two, now using the new threshold computed in step four, keep repeating until the new threshold matches the one before it (i.e. until convergence has been reached).

This iterative algorithm is a special one-dimensional case of the k-means clustering algorithm, which has been proven to converge at a local minimum—meaning that a different initial threshold may give a different final result

4.3 Otsu's method

Otsu's method is used to automatically perform histogram shape-based image thresholding, or, the reduction of a graylevel image to a binary image. The algorithm assumes that the image to be threshold contains two classes of pixels (e.g. foreground and background) then calculates the optimum threshold separating those two classes so that their combined spread (intra-class variance) is minimal. The extension of the original method to multi-level thresholding is referred to as the Multi Otsu method. Otsu's method is named after Nobuyuki Otsu.

In Otsu's method we segment the array I into N classes by means of Otsu's N-thresholding method. otsu returns an array IDX containing the cluster indices (from 1 to N) of each point. Zero values are assigned to non-finite (NaN or Inf) pixels.

IDX = otsu(I) uses N = 2 (default value).

[IDX,sep] = otsu(...) also returns the value (sep) of the separability criterion within the range [0 1]. Zero is obtained only with arrays having less than N values, whereas one (optimal value) is obtained only with N-valued data.

Method

In Otsu's method we exhaustively search for the threshold that minimizes the intra-class variance, defined as a weighted sum of variances of the two classes:

$$\sigma_w^2(t) = \omega_1(t)\sigma_1^2(t) + \omega_2(t)\sigma_2^2(t)$$

Weights ω_i are the probabilities of the two classes separated by a threshold *t* and σ_i^2 variances of these classes.

Otsu shows that minimizing the intra-class variance is the same as maximizing inter-class variance:

$$\sigma_b^2(t) = \sigma^2 - \sigma_w^2(t) = \omega_1(t)\omega_2(t)\left[\mu_1(t) - \mu_2(t)\right]^2$$

which is expressed in terms of class probabilities ω_i and class means μ_i which in turn can be updated iteratively. This idea yields an effective algorithm.

Algorithm

1. Compute histogram and probabilities of each intensity level
2. Set up initial $\omega_i(0)$ and $\mu_i(0)$
3. Step through all possible thresholds $t = 1 \ldots$ maximum intensity
    1. Update ω_i and μ_i
    2. Compute $\sigma_b^2(t)$
4. Desired threshold corresponds to the maximum $\sigma_b^2(t)$

It should be noticed that the thresholds generally become less credible as the number of classes (N) to be separated increases (see Otsu's paper for more details).

If I is an RGB image, a Karhunen-Loeve transform is first performed on the three R,G,B channels. The segmentation is then carried out on the image component that contains most of the energy.

Source Code

```
% Input : f – input image
% Output: BW – segmented image

Function BW= segment(f)
f=im2double(f);
T=0.5*(min(f(:))+max(f(:)));
done=false;
while ~done
   g=f>=T;
   Tn=0.5*(mean(f(g))+mean(f(~g)));
   done=abs(T-Tn)<0.1;
   T=Tn;
end
display('Threshold(T) - Iterative');
T
r=im2bw(f,T);

Th=graythresh(f);
display('Threshold(T) – Otsu''s Method');
Th
s=im2bw(f,Th);

BW = bwareaopen(s, 500);
BW = edge(BW,'canny');
imshow(BW);

[m n] = size(f);

for i=1:m
        for j=1:n
                if(BW(i,j)==1)
                        f(i,j,1)=255;
                end
        end
end
```

4.4 Watershed Transformation

The watershed transformation considers the gradient magnitude of an image as a topographic surface. Pixels having the highest gradient magnitude intensities (GMIs) correspond to watershed lines, which represent the region boundaries. Water placed on any pixel enclosed by a common watershed line flows downhill to a common local intensity minimum (LIM). Pixels draining to a common minimum form a catch basin, which represents a segment.

Source Code

```
% Input: I – input image
% Output: rfgm  - segmented image

function rfgm= segment_watershed(f)
        h=fspecial('sobel');
        fd=im2double(f);
        f= 255-f;
        fd=1 - fd;
        sq=sqrt(imfilter(fd,h,'replicate').^2+imfilter(fd,h','replicate').^2);
        im=imextendedmin(f,100);
        Lim=watershed(bwdist(im));
        em=Lim==0;
        rfmin=imimposemin(sq,im|em);
        wsdmin=watershed(rfmin);
        f= 255-f;
        rfgm=f;
        rfgm(wsdmin==0)=255;
        figure,imshow(rfgm),title('Superimposed - Watershed (GM) and original image');
```

5. Comparison of Different Speckle reducing Methods used:

5.1 Between original Image and noisy images:

Variance	MSE	PSNR
0.002	6.2093	40.2004
0.004	11.8923	37.3781
0.006	16.5881	35.9328
0.008	21.384	34.8299
0.010	25.5054	34.0645
0.012	29.4692	33.4371
0.014	32.8898	32.9602
0.016	36.4112	32.5185
0.018	39.3985	32.176
0.020	42.0052	31.8978

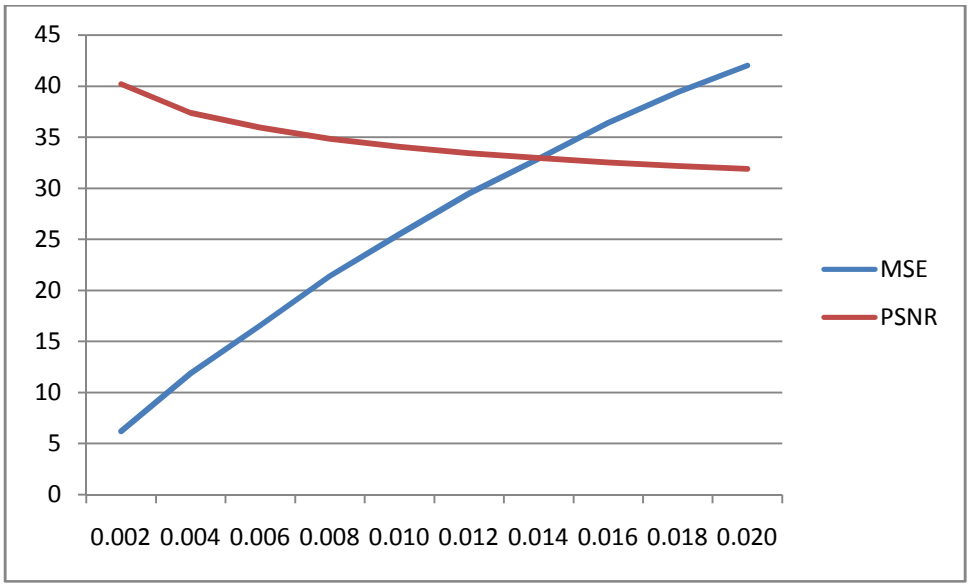

5.2 Between noisy images and SRAD filtered Images:

Variance	MSE	PSNR
0.002	11.7741	37.2568
0.004	15.7722	36.1519
0.006	18.4983	35.4595
0.008	22.1682	34.6735
0.010	26.2689	33.9364
0.012	29.9538	33.3663
0.014	33.8599	32.8339
0.016	37.2801	32.416
0.018	40.9289	32.0105
0.020	43.7161	31.7244

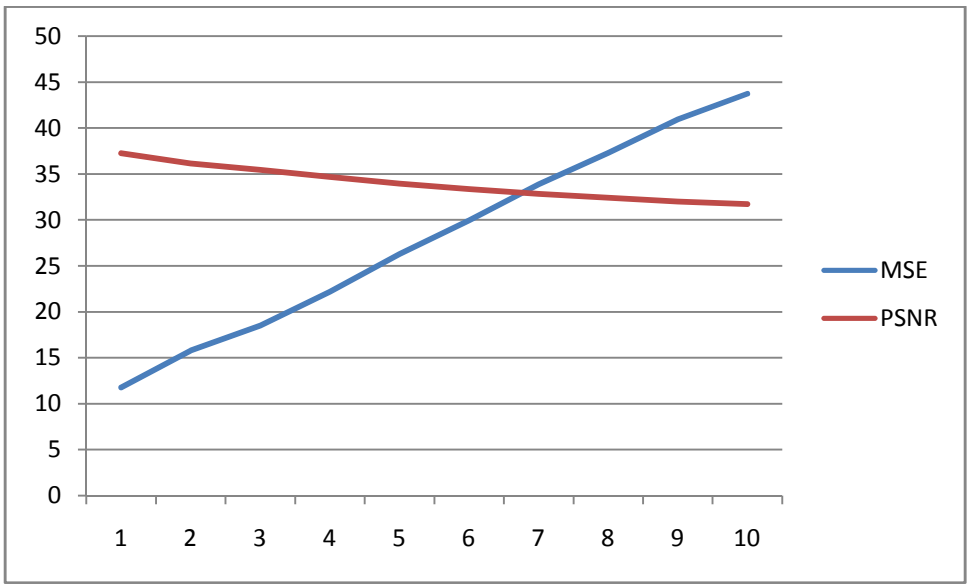

5.3 Between noisy images and LEE filtered Images:

Variance	MSE	PSNR
0.002	13.6466	36.4063
0.004	16.8923	35.9309
0.006	19.5224	35.1592
0.008	21.1827	34.871
0.010	23.4915	34.4217
0.012	26.0312	33.9759
0.014	28.9611	33.5127
0.016	31.3056	33.1746
0.018	33.6592	32.8598
0.020	35.4672	32.6325

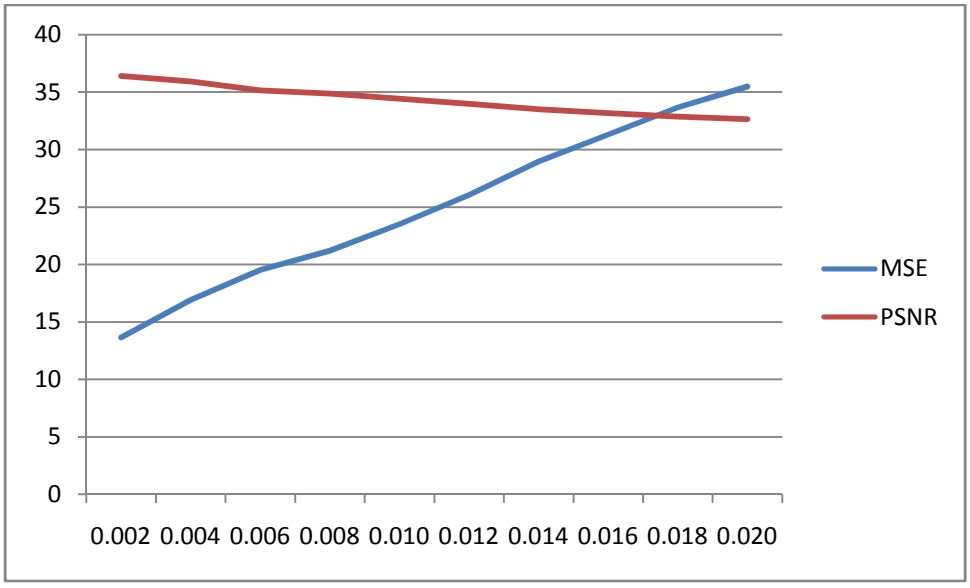

5.4 Between noisy images and FROST filtered Images:

Variance	MSE	PSNR
0.002	11.505	37.4546
0.004	14.5574	36.5
0.006	17.9125	35.5993
0.008	21.7792	34.7504
0.010	25.8929	33.999
0.012	29.7161	33.4009
0.014	33.4292	32.8896
0.016	36.897	32.4609
0.018	40.2993	32.0778
0.020	43.2004	31.7759

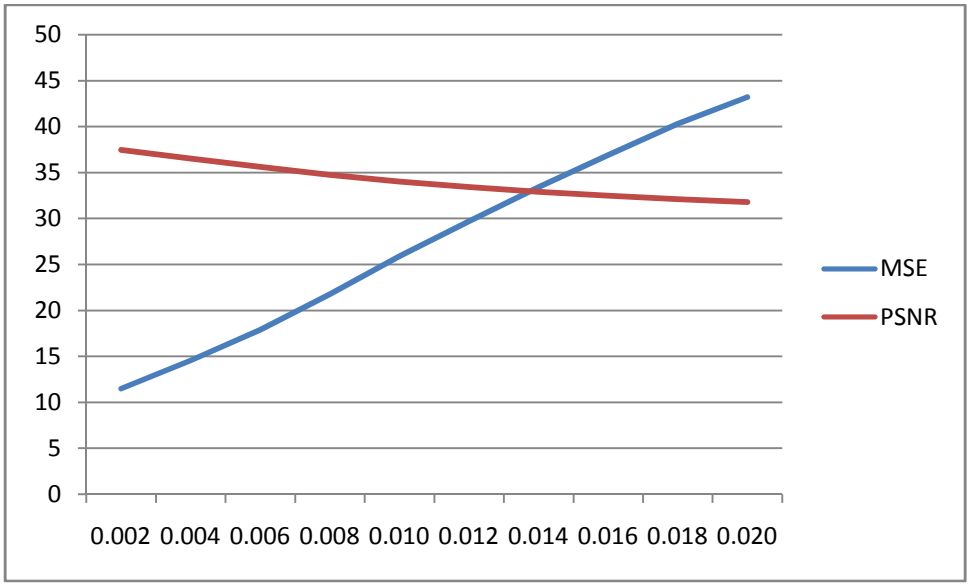

5.5 Between noisy images and PDE filtered Images:

Variance	MSE	PSNR
0.002	13.3646	36.4452
0.004	15.9501	36.1032
0.006	18.4511	35.4706
0.008	22.5234	34.6045
0.010	26.4129	33.9126
0.012	30.5246	33.2843
0.014	34.0312	32.812
0.016	37.4639	32.3947
0.018	41.0758	31.9949
0.020	43.9405	31.7022

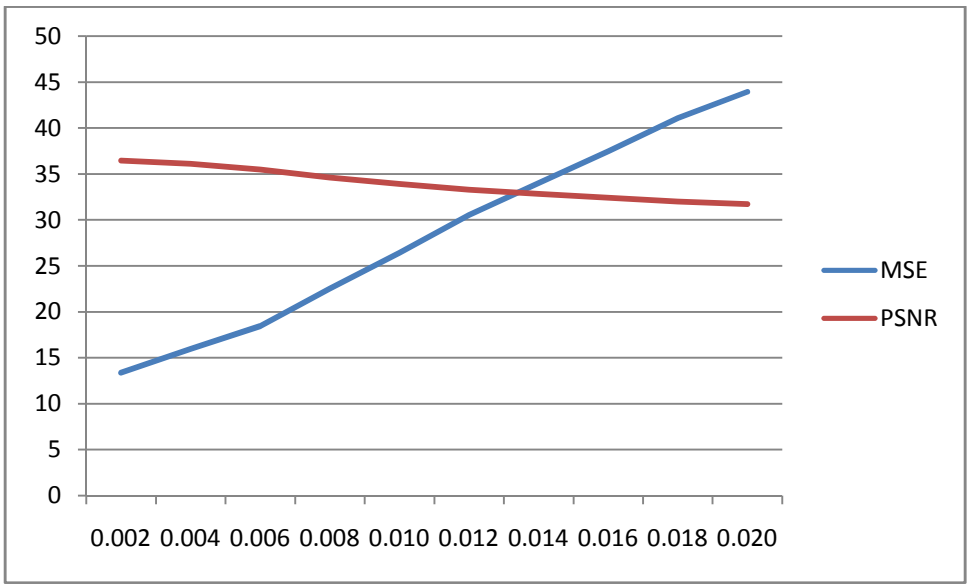

5.6 MSE chart between noisy images and filtered Image by different filtering algorithms:

Variance	srad	lee	frost	PDE
0.002	11.7741	13.6466	11.505	13.3646
0.004	15.7722	16.8923	14.5574	15.9501
0.006	18.4983	19.5224	17.9125	18.4511
0.008	22.1682	21.1827	21.7792	22.5234
0.010	26.2689	23.4915	25.8929	26.4129
0.012	29.9538	26.0312	29.7161	30.5246
0.014	33.8599	28.9611	33.4292	34.0312
0.016	37.2801	31.3056	36.897	37.4639
0.018	40.9289	33.6592	40.2993	41.0758
0.020	43.7161	35.4672	43.2004	43.9405

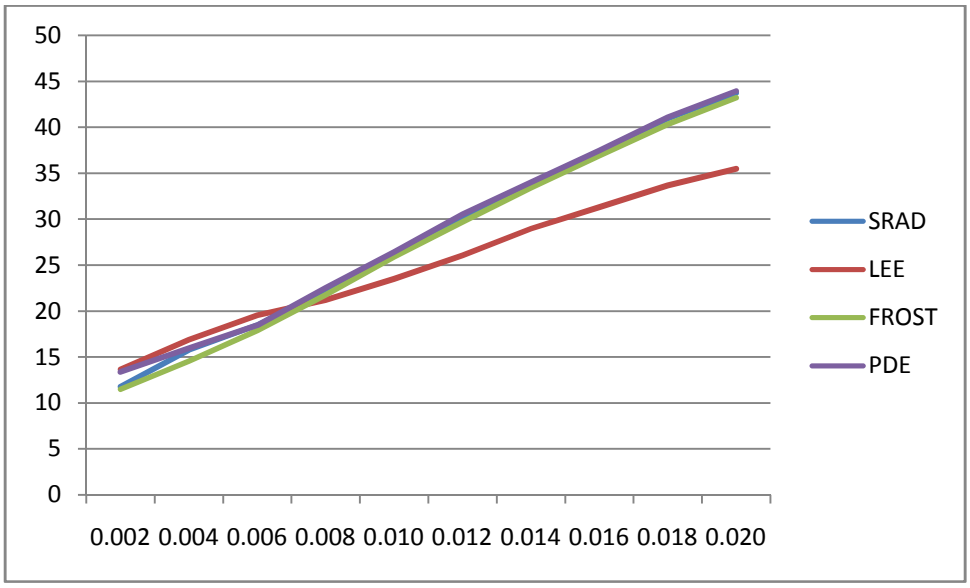

5.7 PSNR chart between noisy images and filtered Image by different filtering algorithms:

Variance	srad	lee	frost	PDE
0.002	37.2568	36.4063	37.4546	36.4452
0.004	36.1519	35.9309	36.5	36.1032
0.006	35.4595	35.1592	35.5993	35.4706
0.008	34.6735	34.871	34.7504	34.6045
0.010	33.9364	34.4217	33.999	33.9126
0.012	33.3663	33.9759	33.4009	33.2843
0.014	32.8339	33.5127	32.8896	32.812
0.016	32.416	33.1746	32.4609	32.3947
0.018	32.0105	32.8598	32.0778	31.9949
0.020	31.7244	32.6325	31.7759	31.7022

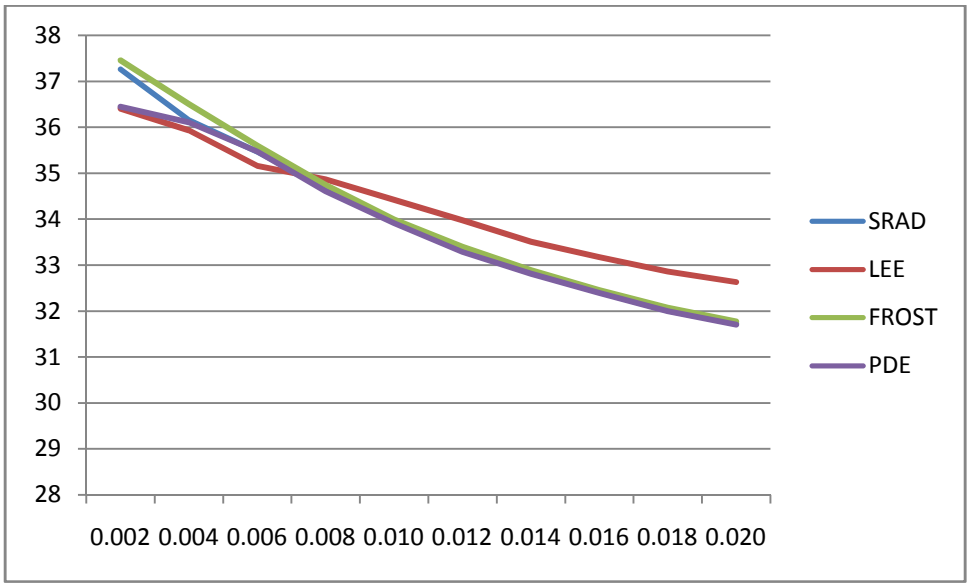

5.8 ISNR chart between noisy images and filtered Image by different filtering algorithms:

Filter	ISNR
SRAD	3.62
LEE	6.7165
FROST	8.5249
PDE	5.113

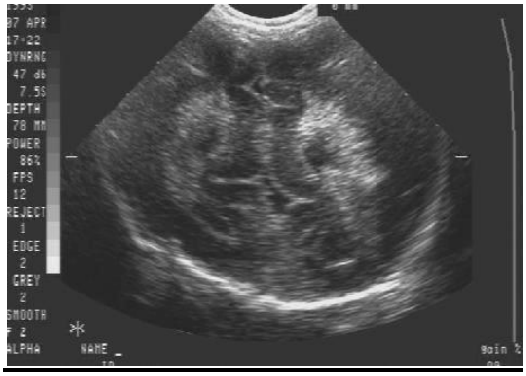

Figure 1. Input noisy image

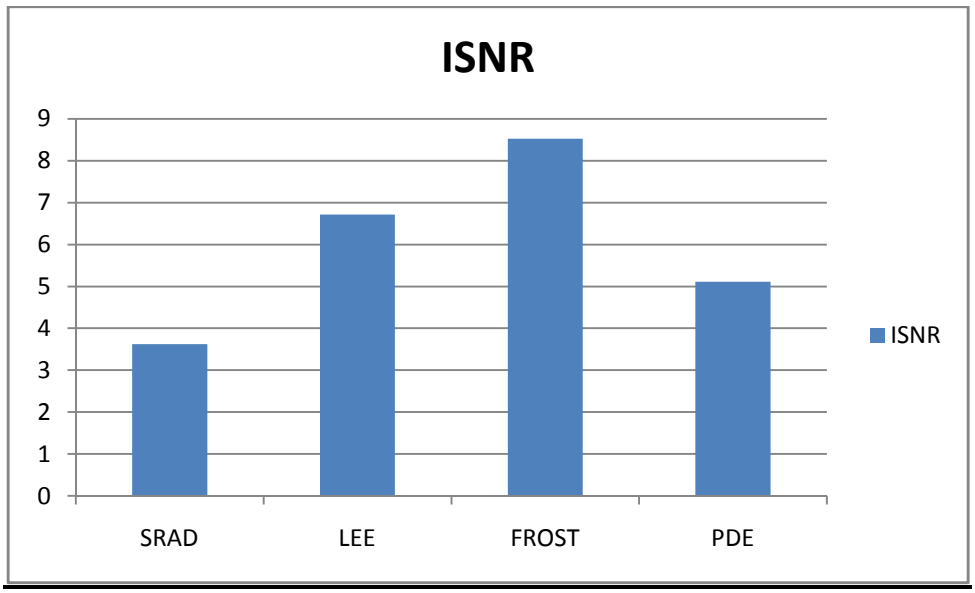

For the given input noisy image we found that the performance of Frost filter is better than SRAD filter, Lee filter and PDE based filter.

6. Conclusion

The filters used for speckle reduction are- SRAD, Frost, Lee, Wiener and Kuan.
Essentially, both the Lee and Kuan filters form an output image by computing a linear combination of the center pixel intensity in a filter window with the average intensity of the window. So, the filters achieve a balance between straightforward averaging (in homogeneous regions) and the identity filter (where edges and point features exist).
The Frost filter also strikes a balance between averaging and the all-pass filter. In this case, the balance is achieved by forming an exponentially shaped filter kernel that can vary from a basic average filter to an identity filter on a point-wise, adaptive basis.
The limitations of these filters are—

- First, the filters are sensitive to the size and the shape of the filter window. If the filter window is too large, over smoothing will occur and edges will be blurred. If the window is small, the smoothing capability of the filter will decrease and the speckles will be left.
- Second, these filters do not enhance edges- they only inhibit smoothing near edges.
- Third, these filters are not directional. In the vicinity of an edge, all smoothing is precluded, instead of inhibiting smoothing in directions perpendicular to the edge and encouraging smoothing in directions parallel to the edge.

Whereas, the PDE-based speckle removal approach (SRAD) allows the generation of an image scale space (a set of filtered images that vary from fine to coarse) without bias due to filter window size and shape. SRAD not only preserves edges but also enhances edges by inhibiting diffusion across edges and allowing diffusion on either side of the edge. SRAD is adaptive and does not utilize hard thresholds to alter performance in homogeneous regions or in regions near edges and small features.
Based on the results obtained we can see that Modified Marker Controlled Watershed transformation produces better results than the two thresholding techniques: Iterative method and Otsu's method.

7. Screenshots

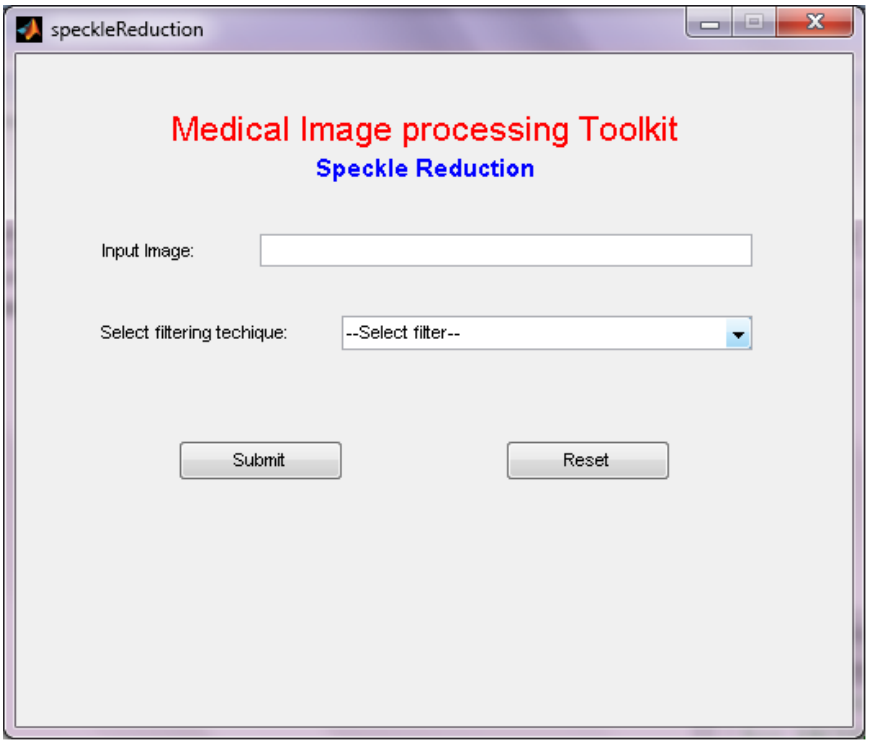

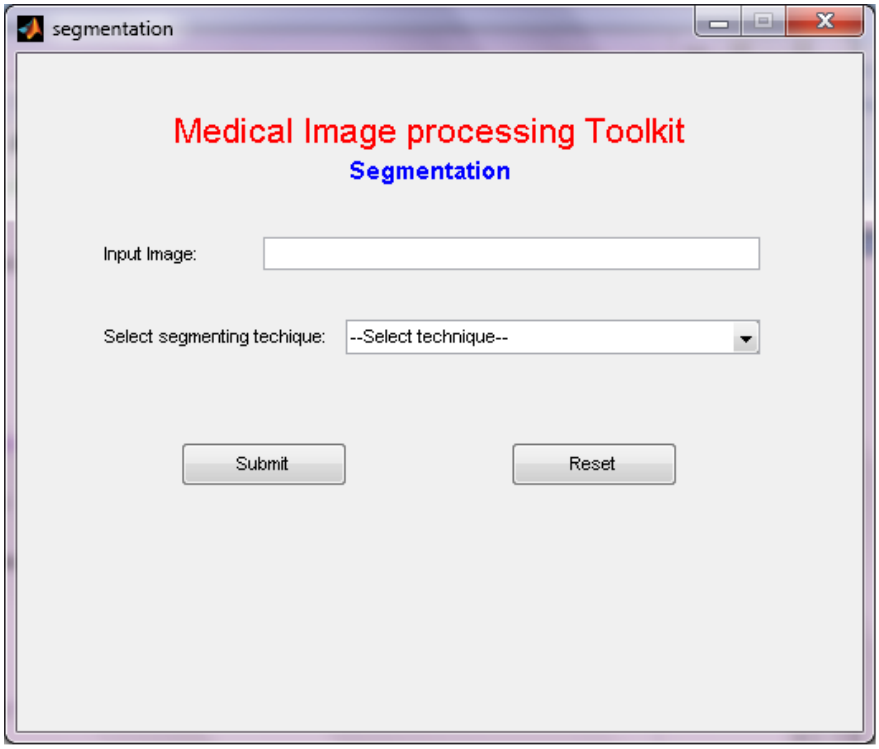

Screenshots of software

References

[1] Society of Nuclear Medicine
[2] Dorland's Medical Dictionary for Health Consumers, 2007 by Saunders; Saunders Comprehensive Veterinary Dictionary, 3 ed. 2007; McGraw-Hill Concise Dictionary of Modern Medicine, 2002 by The McGraw-Hill Companies
[3] Dhawan P, A. (2003). Medical Imaging Analysis. Hoboken, NJ: Wiley-Interscience Publication
[4] Linda G. Shapiro and George C. Stockman (2001): "Computer Vision", pp 279-325, New Jersey, Prentice-Hall
[5] Ron Ohlander, Keith Price, and D. Raj Reddy (1978): "Picture Segmentation Using a Recursive Region Splitting Method", *Computer Graphics and Image Processing*, volume 8, pp 313-333
[6] S. Osher and N. Paragios. Geometric Level Set Methods in Imaging Vision and Graphics, Springer Verlag, ISBN 0387954880, 2003.
[7] Jianbo Shi and Jitendra Malik (2000): "Normalized Cuts and Image Segmentation", IEEE Transactions on pattern analysis and machine intelligence, pp 888-905, Vol. 22, No. 8
[8] Leo Grady (2006): "Random Walks for Image Segmentation", IEEE Transactions on Pattern Analysis and Machine Intelligence, pp. 1768-1783, Vol. 28, No. 11
[9] Z. Wu and R. Leahy (1993): "An optimal graph theoretic approach to data clustering: Theory and its application to image segmentation", IEEE Transactions on Pattern Analysis and Machine Intelligence, pp. 1101-1113, Vol. 15, No. 11
[10] Leo Grady and Eric L. Schwartz (2006): "Isoperimetric Graph Partitioning for Image Segmentation", IEEE Transactions on Pattern Analysis and Machine Intelligence, pp. 469-475, Vol. 28, No. 3
[11] C. T. Zahn (1971): "Graph-theoretical methods for detecting and describing gestalt clusters", IEEE Transactions on Computers, pp. 68-86, Vol. 20, No. 1
[12] Efficient image segmentation using partial differential equations and morphology, Joachim Weickert
[13] Pde-Based Modeling of Image Segmentation using Volumic Flooding by Anastasia Sofou and Petros Maragos
[14] Comparison of PDE based and other techniques for speckle reduction from digitally reconstructed holographic images by Rajeev Srivastav, JRP Gupta and Harish Parthaswamy